مجلة الدراسات التربوية والعلمية - كلية التربية - الجامعة العراقية
العدد الثالث والعشرون - المجلد السادس - علوم الفيزياء - نيسان 2024م
doi.org/10.52866/esj.2023.06.23.09

Study The Optical Properties of Au NPs Prepared by Nd-YAG Laser

Hiba J. Jaafer[a] , Adnan A. Mohammed[b*]
[a] College of Basic Education , University of Diyala, Governorate, Iraq
[b] The general for Education in Diyala, Diyala Governorate, Iraq
*aalmudaris8@gmail.com

Abstract:

In this work, gold nanoparticles (Au) were prepared by pulsed laser ablation technique in deionized water (DW) and sodium bromide borohydride (NaBH4). X-ray diffraction (XRD), ultraviolet and visible spectroscopy (UV-VIS), and Fourier transform infrared spectroscopy (FTIR) were used to characterize produced gold nanoparticles. XRD patterns of Au NP showed that diffraction peaks at angles (2θ~38.33°, 44.62°, 64.69°, and 77.71°), which referred to (111), (200), (220), and (311), favorite directions respectively, these values were corresponded exactly to the international centre for diffraction data (ICDD) card number (00-004-0784)of Au NPs. The UV-VIS was used to analyze the optical properties of the samples, showing peak surface plasmon resonance (SPR) at wavelength (532 nm) in addition to a decrease in energy gap values of (1.75). and 1.61 eV for colloidal solutions (1mM NaBH4 and 2mM NaBH4) compared to colloidal solution (DW). The active groups in the aquatic medium were identified using the FTIR technique, which revealed four significant associations at 3350, 2105, 163.

Keywords: UV-Visible spectroscopy, XRD, FTIR Nd:Yag Laser and pulsed laser ablation technique.

دراسة الخصائص البصرية لحبيبات الذهب النانوية المحضرة بالليزر Nd-YAG

هبة جمعة جعفر[a] ، عدنان علي محمد[b]
[a] كلية التربية الأساسية، جامعة ديالى، محافظة العراق
[b] المديرية العامة لتربية ديالى، محافظة ديالى، العراق

مستخلص:

تم في هذا العمل تحضير حبيبات الذهب النانوية (Au) بواسطة تقنية الاستئصال بالليزر النبضي في محلولي الماء منزوع الايونات (DW) و بروميد الصوديوم بوروهيدريد ($NaBH_4$). تم استخدام حيود الأشعة السينية (XRD)، التحليل الطيفي للأشعة فوق البنفسجية والمرئية (UV-VIS)، والتحليل الطيفي للأشعة تحت الحمراء بتحويل فورييه (FTIR) لتوصيف حبيبات الذهب النانوية المحظرة. أظهرت أنماط XRD لـ (Au NP) أن قمم الحيود عند الزوايا (2θ~ 38.33°, 44.62°, 64.69°, and 77.71°)، المقابلة للمستويات البلورية (111)، (200)، (220)، و (311) على التوالي، كانت هذه القيم تتوافق تمامًا مع رقم البطاقة العالمية (00-004-0784) (ICDD) الخاص بـ Au NPs. تم استخدام جهاز (UV-VIS) لتحليل الخصائص البصرية للعينات، حيث أظهرت ذروة رنين البلازمون السطحي (SPR) عند الطول الموجي (532 nm) بالإضافة إلى انخفاض في قيم فجوة الطاقة بمقدار (1.75 and 1.61 eV) للمحاليل الغروية ($1mM\ NaBH_4$ and $2mM\ NaBH_4$) مقارنة بالمحلول الغروي (DW). تم تحديد المجموعات النشطة في الوسط المائي باستخدام تقنية FTIR، والتي كشفت عن أربع روابط معنوية عند 3350, and 671 cm^{-1}, 2105, 1635.

الكلمات المفتاحية: التحليل الطيفي للأشعة فوق البنفسجية والمرئية، XRD، FTIR ، ليزر Nd:Yag - تقنية الاستئصال بالليزر النبضي.

1. Introduction

Noble metal nanoparticles (NPs) are important key sources in multiple fundamental and applied study fields, including, but not limited to, catalysis, optics, fuel cell research, and medicine [1]. Metallic NPs are an essential subset of this NP family because of their specialized uses in the biomedical [2-4], optical [5,6], and electronic [6,7] sectors, as well as their potential as performance-enhancing additives in concrete [8,9]. The size and shape of these NPs play a significant role in achieving the desired characteristics [10,11]. Consequently, for the synthesis of nanomaterials, several techniques have been developed, such as physical [12,13], chemical [14], and biological [15] approaches. A new technique called laser ablation of solid targets in liquid has been developed[16]. Due to the fact that this technique depends on ablating a solid object in a liquid, it can be applied in a single stage, and a variety of liquid media types can be used as long as they are transparent to the laser beam. Preparing metal nanoparticles in solutions presents a significant challenge due to the lack of direct control over the nanoparticles' size and form [17]. At the nanoscale, the ratio of surface area to volume is high.Therefore, reducing the size of NPs has the potential to modify many of their physical, chemical, and biological properties [18,19]. In particular, Au NPs are useful in many different areas [20-22] due to their biocompatibility and non-cytotoxicity, making them a superior option when compared to other metal nanoparticles. Here, ultra-fine Au NPs were produced by laser ablation of a solid Au object in liquid, with sodium borohydride serving as a surfactant. The chemical substance sodium borohydride (NaBH4) is frequently used as a potent reducing agent. As a result of the adsorption of borohydride ions, electrostatic repulsion should act between the nanoparticles to keep them suspended [14,23]. Compared to other ionic detergents like sodium dodecyl sulfate (SDS), cetyl trimethylammonium bromide (CTAB), and ethylene glycol, sodium borohydride is more cost-effective.

2. Procedure

2.1 Synthesis of Gold Nanoparticles (Au NPs) by laser ablation (PLA)

Laser ablation (PLA) of a gold alloy was used to synthesize gold nanoparticles, and gold (as a target) was put at the bottom of a glass beaker vessel containing (3 ml) of solutions (distilled water (DW) and (1mM, 2mM) of sodium bromide borohydride ($NaBH_4$), the nanoparticles basics for pulsed laser Nd- YAG used Wave length (λ=1064 nm), Frequency (f =3 Hz), Energy (E= 500 Mj) and number of pulses (n= 500 pulses).

2.2 Diagnosis of nanoparticles

The FTIR characteristics of Au nanoparticles were investigated using an Affinty-1CE spectrophotometer. The X-ray diffraction device used in this study was of the type (Shimadzu-6000) of Japanese origin. The UV-VIS spectrometer (made by Shimadzu, Japan) was utilized to capture the colloids' surface Plasmon resonance and absorption spectra. At room temperature.

3. Data, value and validation

3.1 The XRD analysis

The XRD patterns of gold nanoparticles produced by a pulsed Nd:YAG laser are shown in Figure 1. It was found that the diffraction peaks are (38.33°, 44.62°, 64.69°, and 77.71°), which correspond to the desired directions (111), (200), (220), and (311), respectively. These numbers are in perfect accord with the international centre for diffraction data (ICDD) number (00-004-0784) of Au NPs', and the results also support [24].

The Scherrer method was used to determine the average crystallite size of the produced nanoparticles [25]:

$$D = \left(\frac{k\lambda}{\beta \cos\theta}\right) \quad \text{.....(1)}$$

where D is the crystallite size, K is a constant (equal to 0.94), λ is the wavelength of the x-ray radiation, β is the full width at half maximum and θ is the angle of diffraction. The results showed that the crystal size ranged between (8.77 and 13.46 nm), as shown in Table 1.

Table 1: Data for the X-ray diffraction of Au NPs.

2θ (deg.)	FWHM (deg.)	(hkl)	D (nm)
38.33	0.57	(111)	13.46
44.62	0.87	(200)	8.77
64.69	0.76	(220)	9.15
77.71	0.61	(311)	10.58

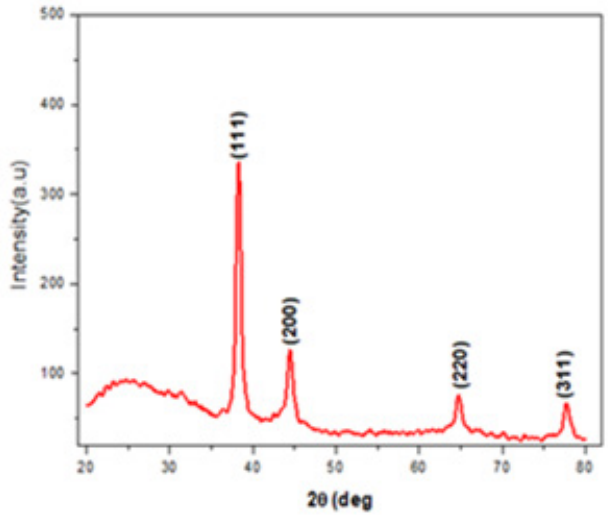

Figure 1. XRD patterns of Au NPs.

3-2 Spectra of UV-VIS Absorption and Calculation of the Energy Gap

Figure 2 shows the UV- VIS) ، spectrum obtained by (PLA) in solutions deionized water (DW), 1 mill moles (mM) NaBH4 and 2mM NaBH4), respectively. While figure (3) depicts the position of the gold nanoparticles' surface plasmon peak at approximately 532 nm and the absorbance (0.08) at roughly the same wavelength, nanoparticles have formed and this is explained by the absorption of Au nanoparticles caused by the interband transition. In noble metals, electrons can transfer from the conduction band far above Fermi level, producing inter - band absorption at shorter wavelengths. [19]. Even though ($NaBH_4$) absorption peak narrowed and moved toward shorter wavelengths, borohydride's absorption peak showed no discernible change [26, 27]. In Table (2), we can see the energy difference, surface plasmon resonance, and absorption of gold nanoparticles. Using Tauc's method [28], It is possible to measure the energy-gap of the (Au) nanoparticles. from the absorption spectra.

$$(\alpha h\upsilon)^{n} = B\,(h\upsilon - E_g) \quad \ldots\ldots\ldots\ldots\ldots (2)$$

Where B: Planck's constant,

ν: photon frequency,

hν: photon energy,

Eg: energy gap,

n: exponent which can have values of either 2 or 1/2 for direct transmission and for indirect transmission respectively, and α : the absorption coefficient (cm^{-1}), which was calculated using the formula αd = ln (1/T), where

d stands for the wave's path length (in cm) and was set to be equal to the cuvette's length of 1 cm. Using the measured absorbance (A_λ) at the wavelength of light (λ), the transmittance was computed using [29]:

$$A_\lambda = -\log 10(T) \text{ .....(3)}$$

The optical energy gap edge of the produced nanoparticles in solution ($NaBH_4$) rises in comparison to the optical energy gap edge of deionized distilled water due to the impact of quantitative confinement. Hence, creating tiny particles is acceptable for the bigger energy gap [29].

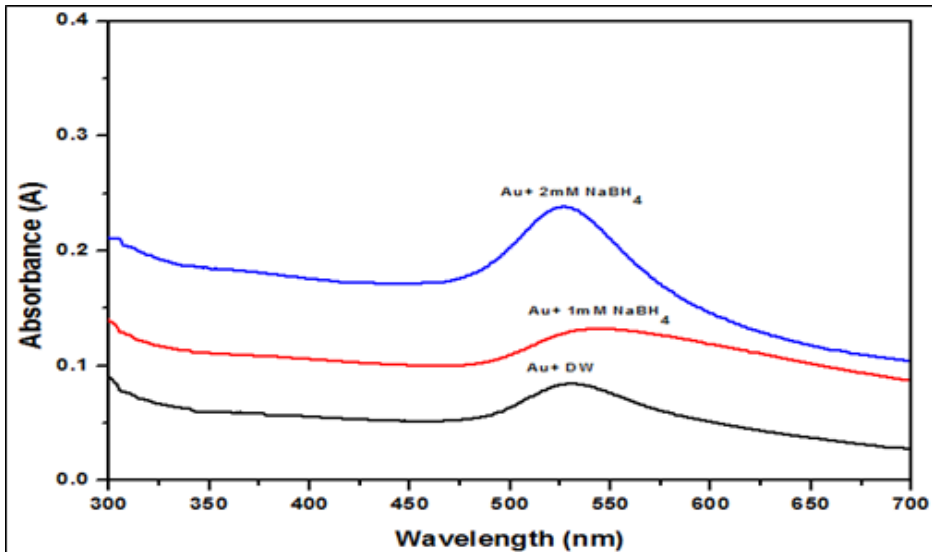

Fig. (2): UV-Visible absorption spectra of colloidal gold nanoparticles.

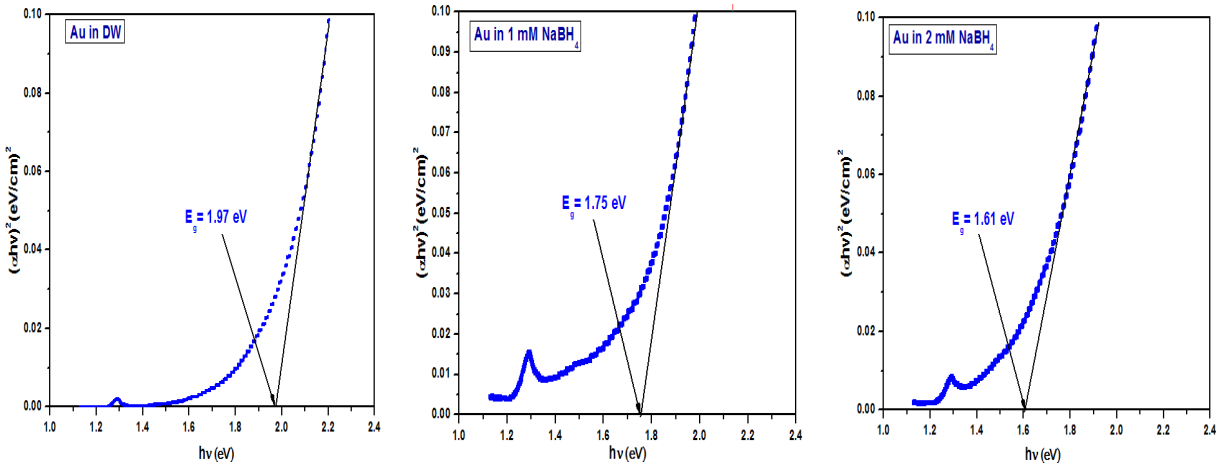

Fig. (3): Colloidal gold nanoparticle samples' direct band gap calculations.

Table (2): The absorption, surface Plasmon resonance and energy gap values of gold nanoparticles.

Nanoparticle Types	Absorption (a.u)	Surface Plasmon Resonance SPR(nm)	Eg(eV)
Au+(DW)	0.08	532	1.97
Au+ 1mM NH_4	0.13	530	1.75
Au+ 2mM NH_4	0.24	525	1.61

3.2 FTIR Analysis

(FTIR) spectrum is commonly employed for studying chemical interactions in materials. In this studed, FTIR spectroscopy was used to examine a liquid containing gold nanoparticles between 400 and 4500 cm^{-1}. As shown in the figure, the FTIR spectra of the materials revealed four dips at 3350, 2105, 1635, and 671 cm^{-1}. In water, the O-H stretching vibration model can explain the dip at 3350 cm^{-1} [29]. In a similar vein, the trough at 2105 cm^{-1} is ascribed to the carbon-carbon triple bond C=C [30, 31], and the trough at 1635 cm^{-1} is due to the aromatic C=C vibrations [32]. Lastly, the dip at 671 cm^{-1} is associated with the C-H bond [33]. Figure (4) shows that when surfactants ($NaBH_4$) were used to coat Au NP_s, the absorbance stretch of the strong hydroxyl group became high-curved compared to (DW), and bonds narrowed and sharpened for (Au NPs) particles prepared with ($NaBH_4$) compared to uncoated (DW) particles.

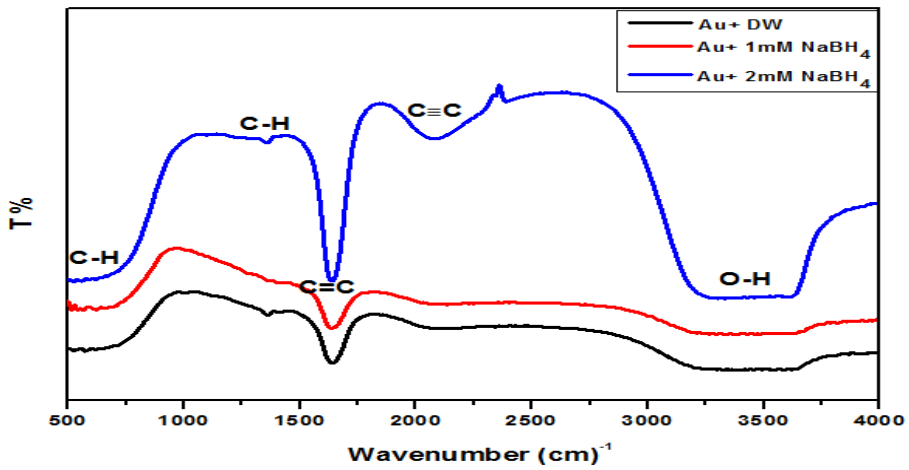

Fig.(4): FTIR spectrums of gold nanoparticle prepared in solutions (DW, 1mM $NaBH_4$, 2mM NaBH4)

4. Conclusions

Based on the aforementioned results, it was found that it is possible to prepare gold nanoparticles using the pulsed laser ablation (PLA) method, which is a clean and easy-to-use technique. Various techniques such as UV-VIS and FTIR) were used to characterize the nanoparticles. The absorption spectrum of all the prepared colloidal solutions showed strong resonance on the plasmon surface. (AuNPs) with a good energy gap. While the measurement (FTIR) showed that the bonds become sharper at 2) mm NaBH4) compared to the colloidal solution (DW).

References

1. Speder J, Altmann L, Roefzaad M, BäumerM, Kirkensgaard JJK, Mortensen K, Arenz M, Pt based PEMFC catalysts prepared from colloidal particle suspensions-a toolbox for model studies. Phys Chem Chem Phys, (2013). 15(10): pp.3602–3608.
2. Díaz-Visurraga, J., Gutiérrez, C., Von Plessing, C., & García, A., Metal nanostructures as antibacterial agents, in Science against Microbial Pathogens: Communicating Current Research and Technological Advances, Formatex Research Center: Spain, 2011. 1: pp. 210-218.
3. Li, W. R., Xie, X. B., Shi, Q. S., Duan, S. S., Ouyang, Y. S., & Chen, Y. B., Antibacterial effect of silver nanoparticles on Staphylococcus aureus. Research in microbiology, 2011. 162(5): pp. 542-549.
4. Rana, S. and P. Kalaichelvan, Antibacterial activities of metal nanoparticles. Adv. Biotech, 2011. 11(2): pp. 21-23.
5. Smitha, S. L., Nissamudeen, K. M., Philip, D., & Gopchandran, K. G, Studies on surface plasmon resonance and photoluminescence of silver nanoparticles. Spectrochimica Acta Part A: Molecular and Biomolecular Spectroscopy, 2008. 71(1): pp. 186-190.
6. Le Guével, X., Wang, F. Y., Stranik, O., Nooney, R., Gubala, V., McDonagh, C., & MacCraith, B. D., Synthesis, stabilization, and functionalization of silver nanoplates for biosensor applications. The Journal of Physical Chemistry C,

2009. 113(37): pp. 16380-16386.
7. Zhu, S., C. Du, and Y. Fu, Fabrication and characterization of rhombic silver nanoparticles for biosensing. Optical Materials, 2009. 31(6): pp. 769-774.
8. Reches, Y., Nanoparticles as concrete additives: Review and perspectives. Construction and Building Materials, 2018. 175: pp. 483-495.
9. Sanchez, F. and K. Sobolev, Nanotechnology in concrete–a review. Construction and Building Materials, 2010. 24(11): pp. 2060-2071.
10. Semaltianos, N., Nanoparticles by laser ablation. Critical Reviews in Solid State and Materials Sciences, 2010. 35(2): pp. 105-124.
11. Bae, C.H., S.H. Nam, and S.M. Park, Formation of silver nanoparticles by laser ablation of a silver target in NaCl solution. Applied Surface Science, 2002. 197-198: pp. 628-634.
12. Tsuji, T., et al., *Preparation of silver nanoparticles by laser ablation in solution: influence of laser wavelength on particle size.* Applied Surface Science, 2002. 202(1) : pp. 80-85.
13. Omurzak, E., et al., *Wurtzite-type ZnS nanoparticles by pulsed electric discharge.* Nanotechnology, 2011. 22(36): pp. 1-7.
14. Jeong, Y., D.W. Lim, and J. Choi, *Assessment of size-dependent antimicrobial and cytotoxic properties of silver nanoparticles.* Advances in Materials Science and Engineering, 2014. 9065: pp. 1-6.
15. Philip, D., *Green synthesis of gold and silver nanoparticles using Hibiscus rosa sinensis.* Physica E: Low-Dimensional Systems and Nanostructures, 2010. **42**(5): pp. 1417-1424.
16. Neddersen, J., G. Chumanov, and T.M. Cotton, *Laser ablation of metals: a new method for preparing SERS active colloids.* Applied Spectroscopy, 1993. 47(12): pp. 1959-1964.
17. Olea-Mejía, O., et al., *Silver Nanoparticles Obtained by Laser Ablation Using Different Stabilizers.* Japanese Journal of Applied Physics, 2013. 52(11NJ01): pp. 1-6.
18. Hannink, R.H. and A.J. Hill, *Nanostructure control of materials*. 2006, New York Washington, DC:

Woodhead Publishing.

19. Takeshima, T., et al., *DNA/Ag nanoparticles as antibacterial agents against gram-negative bacteria.* Nanomaterials, 2015. **5**(1): pp. 284-297.
20. Corma, A. and H. Garcia, Supported gold nanoparticles as catalysts for organic reactions. Chemical Society Reviews, 2008. 37(9): pp. 2096-2126.
21. Ahirwal, G.K. and C.K. Mitra, Direct electrochemistry of horseradish peroxidase-gold nanoparticles conjugate. Sensors, 2009. 9(2): pp. 881-894.
22. Schmid, G. and U. Simon, Gold nanoparticles: assembly and electrical properties in 1–3 dimensions. Chemical Communications, 2005(6): pp. 697-710.
23. Van Dong, P., C.H. Ha, and J. Kasbohm, Chemical synthesis and antibacterial activity of novel-shaped silver nanoparticles. International Nano Letters, 2012. 2(1): pp. 1-9.
24. Ali, H. S., Fakhri, M. A., & Khalifa, Z.. Optical and structural properties of the gold nanoparticles ablated by laser ablation in ethanol for biosensors. In Journal of Physics: Conference Series, IOP Publishing, 2021. 1795 (1), pp. 1-7.
25. Mohammed, A. A., Khodair, Z. T., & Khadom A. A, Preparation, characterization and application of Al_2O_3 nanoparticles for the protection of boiler steel tubes from high temperature corrosion. Ceramics International, 2020. 46(17), p.p. 26945-26955.
26. V. Nguyen, L. Yan, J. Si and X. Hou, "Femtosecond Laser Induced Size Reduction of Carbon Nanodots in Solution: Effect of Laser Fluence Spot Size and Irradiation Time", Journal of Applied Physics, 2015. 117, pp. 1-6.
27. R. Baiee, Z. Liu and L. Li, "Production of Ultra-Fine Ag Nanoparticles by Laser Ablation in Diluted Sodium Borohydride Solution and Their Antibacterial Properties", International Journal of Nanoparticles and Nanotechnology, 2018. 4, pp. 2631-5084.
28. S. Dagher, Y. Haik, A. I. Ayesh and N. Tit, "Synthesis and Optical Properties of Colloidal CuO Nanoparticles", Journal of Luminescence, 2004. 151, pp.149-154.

29. D. Dorranian, E. Solati and L. Dejam, “Photoluminescence of ZnO Nanoparticles Generated by Laser Ablation in Deionized Water”, Applied Physics A , Materiales Science &Processing, , 2012. 109, pp. 307- 314.
30. J. Yan, M. J. Uddin, T. j. Dickens, O. I. Okoli, “Carbon Nanotubes (CNTs) Enrich the Solar Cells”, Solar Energy, 2013. 96, pp. 239-252.
31. K. S. Novoselov, A. K. Geim, S. V. Morozov, D. Jiang, Y. Zhang, S. V. Dubonos, I. V. Grigorieva and A. Firsov, “Electric Field Effect in Atomically Thin Carbon Films”, Science, 2004. 306, pp. 666- 669.
32. E. Vaghri and D. Dorranian, “Effect of Ablation Environment on the Characteristics of Grapheme Nanosheets Produced by Laser”, Studia Ubb Chemia, 2016, 61.4: 277-285.
33. Z. M. Sui, X. Chen, L. M. Xu, W. C. Zhuang, Y. C. Chai and C. J. Yang, “Capping Effect of CTAB on Positively Charged Ag Nanoparticles”, Physica E, 2006, 33.2: 308-314.